Cu_2O_2 Equilibrium

DOI: 10.1002/anie.201402166

Observation of a Cu^{II}_2(μ-1,2-peroxo)/Cu^{III}_2(μ-oxo)$_2$ Equilibrium and its Implications for Copper–Dioxygen Reactivity**

Matthew T. Kieber-Emmons, Jake W. Ginsbach, Patrick K. Wick, Heather R. Lucas, Matthew E. Helton, Baldo Lucchese, Masatatsu Suzuki, Andreas D. Zuberbühler, Kenneth D. Karlin, and Edward I. Solomon**

Abstract: *Synthesis of small-molecule Cu_2O_2 adducts has provided insight into the related biological systems and their reactivity patterns including the interconversion of the Cu^{II}_2(μ-η^2:η^2-peroxo) and Cu^{III}_2(μ-oxo)$_2$ isomers. In this study, absorption spectroscopy, kinetics, and resonance Raman data show that the oxygenated product of $[(BQPA)Cu^{I}]^+$ initially yields an "end-on peroxo" species, that subsequently converts to the thermodynamically more stable "bis-μ-oxo" isomer ($K_{eq} = 3.2$ at −90°C). Calibration of density functional theory calculations to these experimental data suggest that the electrophilic reactivity previously ascribed to end-on peroxo species is in fact a result of an accessible bis-μ-oxo isomer, an electrophilic Cu_2O_2 isomer in contrast to the nucleophilic reactivity of binuclear Cu^{II} end-on peroxo species. This study is the first report of the interconversion of an end-on peroxo to bis-μ-oxo species in transition metal-dioxygen chemistry.*

Dioxygen binding and activation by hemocyanin, catechol oxidase, tyrosinase, and hydroxy-anilinase[1] have inspired exploration of the preparative chemistry and structure–function correlations of small-molecule Cu_2O_2 adducts.[2] Only the "side-on peroxo" (Cu^{II}_2(μ-η^2:η^2-peroxo)) binding motif has been observed in these enzymes,[1] while two additional structural types are commonly found in small-molecule adducts: "end-on peroxo" (Cu^{II}_2(μ-1,2-peroxo)) and "bis-μ-oxo" (Cu^{III}_2(μ-oxo)$_2$) isomers (Figure 1).[2] The side-on peroxo and bis-μ-oxo species have been found to be in equilibrium, suggesting the possibility of either functioning as the electrophile in tyrosinase that *o*-hydroxylates phenol during catalysis. Indeed, both mechanistic possibilities are supported by model studies.[3] In contrast, the end-on peroxo species typically behaves as a nucleophile.[2d,4]

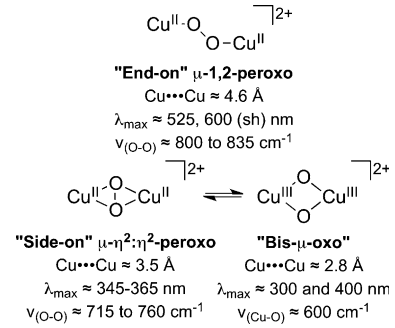

Figure 1. Cu_2O_2 isomers.

Thus, we were intrigued by a recent report of phenolate *ortho*-hydroxylation by an end-on peroxo adduct,[5] a reaction otherwise believed to proceed through electrophilic aromatic substitution.[3a,d] This led us to consider the possible involvement of an unobserved bis-μ-oxo species that possesses the electrophilic character needed to affect a phenol-to-catechol conversion.

Presented here is a reevaluation of the chemistry of a binuclear $Cu_2(O_2)$ complex that employs the tripodal amine scaffold, bis(2-quinolylmethyl)-(2-pyridylmethyl)amine (BQPA, Figure 2),[7] that explicitly demonstrates, for the first time, an end-on peroxo to bis-μ-oxo equilibrium, deduced from UV/Vis and resonance Raman (rR) spectroscopies. The calibration of density functional theory (DFT) calculations to experimental thermodynamic data support involvement of a bis-μ-oxo rather than an end-on peroxo species as the electrophile in the reported[5] phenolate hydroxylation.

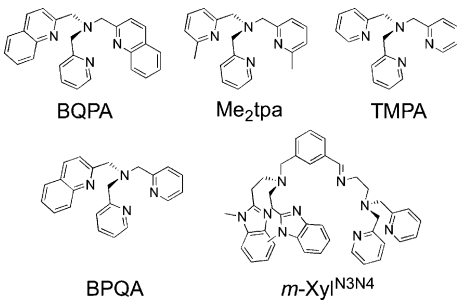

Figure 2. Ligand scaffolds.

[*] Dr. M. T. Kieber-Emmons, J. W. Ginsbach, Prof. E. I. Solomon
Department of Chemistry, Stanford University
Stanford, CA 94305 (USA)
E-mail: edward.solomon@stanford.edu
Dr. H. R. Lucas, Dr. M. E. Helton, Dr. B. Lucchese, Prof. K. D. Karlin
Department of Chemistry, The Johns Hopkins University
Baltimore, MD 21218 (USA)
E-mail: karlin@jhu.edu
Dr. P. K. Wick, Prof. A. D. Zuberbühler
Department of Chemistry, University of Basel
4056 Basel (Switzerland)
Prof. M. Suzuki
Division of Material Sciences, Kanazawa University
Kakuma-machi, Kanazawa 920-1192 (Japan)

[**] These studies were supported by the NIH (DK031450 to E.I.S.; GM60353 to K.D.K.; postdoctoral fellowship GM085914 to M.K.E.).
Supporting information for this article is available on the WWW under http://dx.doi.org/10.1002/anie.201402166.

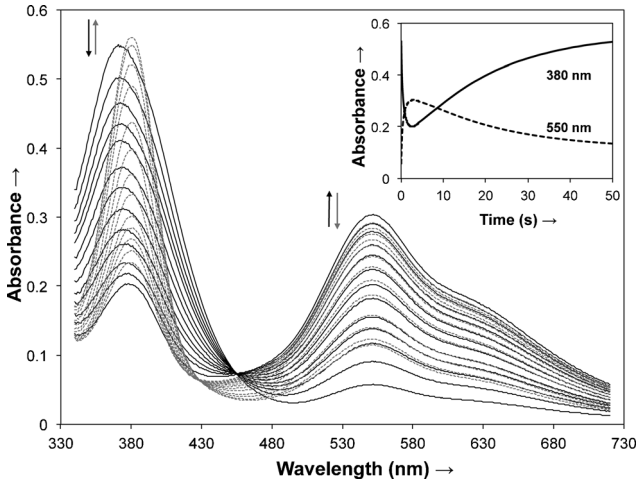

Figure 3. Time-dependent UV/Vis spectra (207 s) for the oxygenation of $[(BQPA)Cu^{I}]^{+}$ **1** in THF at −98.6 °C and absorbance–time traces at 380 nm and 550 nm (insert). Initially, the 370 nm band of **1** decays as the spectral features of **2** forms (——) followed by the decay of **2** and the growth of **3** (-----).

Following earlier investigations into the O_2 reactivity of $[(BQPA)Cu^{I}]PF_6$ in EtCN,[7,8] Figure 3 illustrates the UV/Vis spectroscopic progression of the reaction of $[(BQPA)Cu^{I}]B(C_6F_5)_4$ **1** with O_2 in THF. Initially, complex **2** with 545 and 620 (sh) nm features forms rapidly and has a similar absorption spectrum to those of previously characterized end-on peroxo species.[9] Within a few seconds, **2** begins converting to species **3** with an intense 380 nm band. However the transformation is not complete, but rather approaches an equilibrium mixture of **2** and **3** in approximately a 1:3 ratio.

The structure of the oxygenated species **2** and **3** were further probed by rR spectroscopy. Excitation of a solution that contains mostly **2** with 568 nm laser radiation resulted in the observation of four apparent oxygen isotope sensitive features clustered in two distinct regions, 835 cm^{-1} and 821 cm^{-1} ($^{18}O_2$: 793 cm^{-1} and 777 cm^{-1}) and 542 cm^{-1} and 504 cm^{-1} ($^{18}O_2$: 521 cm^{-1} and 488 cm^{-1}, Figure 4). The former

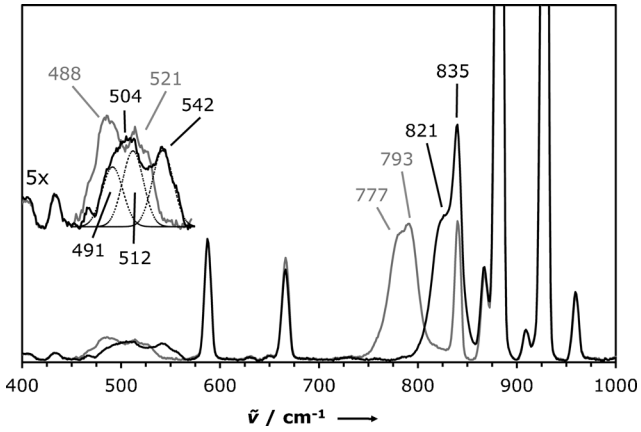

Figure 4. Resonance Raman spectra of **2**, prepared with natural-abundance O_2 (black curve) and $^{18}O_2$ (gray curve) with 568 nm excitation in THF. Inset: Spectrum scaled 5×.

region is consistent with the intraperoxide stretch (νO–O) and the later is consistent with metal-ligand stretch (νCu–O) of an end-on peroxide core.[9,10] Excitation of a frozen solution of mostly **3** with 380 nm laser light enhanced an oxygen isotope sensitive feature at 584 cm^{-1} ($^{18}O_2$: 560 cm^{-1}) (Figure 5).

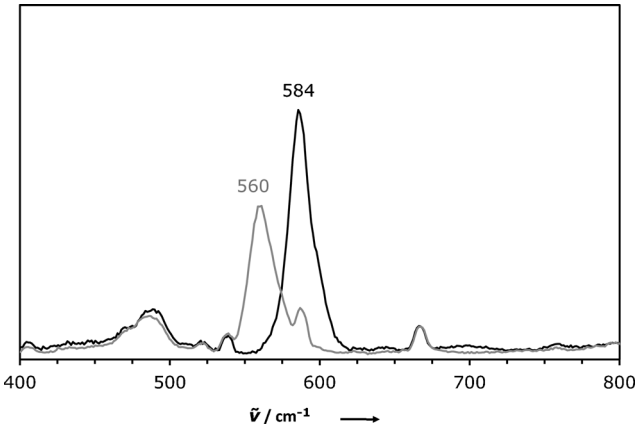

Figure 5. Resonance Raman spectra of **3** prepared with natural-abundance O_2 (black curve) and $^{18}O_2$ (gray curve) with 380 nm excitation in THF.

Based on its energy and isotope shift, this feature is assigned as the symmetric νCu–O breathing mode of a bis-μ-oxo species; a similar rR spectrum was observed for the crystallographically characterized $[\{(Me_2tpa)Cu^{III}\}_2(\mu\text{-}O)_2]^{2+}$ (Figure 2).[11] These results indicate that the two oxygenated products of $[(BQPA)Cu^{I}]^{+}$ that are in equilibrium are an end-on peroxo (**2**) and a bis-μ-oxo species (**3**) (Figure 6).[12]

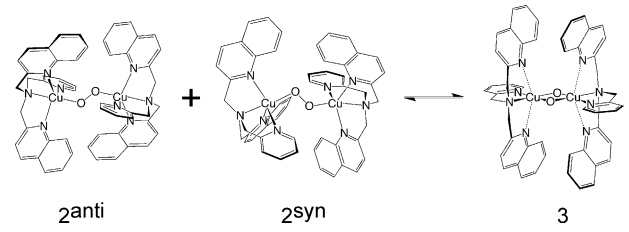

Figure 6. End-on peroxo/bis-μ-oxo isomerization.

The detailed assignment of the rR spectra of **2** is complicated by the observation of two νO–O features. This suggested the presence of two peroxo adducts, attributed to the non-symmetric BQPA ligand that would lead to two possible orientations of the pyridyl substituent in the interdigitated dimer (Figure 6), C_1 symmetric "syn" ($\mathbf{2}^{syn}$) and overall C_i symmetric "anti" ($\mathbf{2}^{anti}$) that contains a C_{2h} Cu_2O_2 core. DFT calculations on these two isomers indicate that $\mathbf{2}^{anti}$ is favored by approximately 3 kcal mol^{-1} (Supporting Information, Table S9). Group theory considerations predict that in the effective C_{2h} symmetry ($\mathbf{2}^{anti}$), only the $\nu Cu–O_{sym}$ vibration transforms as A_g and would be allowed, whereas in C_1 symmetry ($\mathbf{2}^{syn}$) both $\nu Cu–O_{sym}$ and $\nu Cu–O_{antisym}$ trans-

form as A leading to a total of three expected features in the metal ligand stretching region. For the Cu–O region, two transitions with comparable intensity are observed (Figure 4). In other end-on peroxo complexes, two metal-ligand features are observed and are assigned as dimer $\nu Cu–O_{sym}$ and dimer $\nu Cu–O_{antisym}$ bands at higher and lower energy, respectively, with the symmetric stretch enhanced relative to the weaker antisymmetric stretch.[6a,13] In the rR spectrum of **2**, the lower energy metal-ligand feature is more intense than the higher energy feature, inconsistent with a simple assignment as the $\nu Cu–O_{antisym}$ stretch. Bandshape analysis of the oxygen isotope sensitive features in the metal ligand stretching region are best fit by three bands with the same bandwidth at 542 cm^{-1}, 512 cm^{-1} and 491 cm^{-1} giving an intensity ratio of 1.0:1.0:0.8. Analytical frequency calculations from the DFT structures (see Supporting Information) indicate that the 835 cm^{-1} and 542 cm^{-1} features correspond to $\mathbf{2}^{anti}$ (the $\nu O–O$ and $\nu Cu–O_{sym}$, respectively) while the 821 cm^{-1}, 512 cm^{-1}, and 491 cm^{-1} features arise from $\mathbf{2}^{syn}$ (the $\nu O–O$, $\nu Cu–O_{sym}$, and $\nu Cu–O_{antisym}$, respectively).

Additional quantitative information on the nature of the end-on peroxo/bis-μ-oxo equilibrium was determined from modeling stopped-flow kinetics data of the reaction of $[(BQPA)Cu^{I}]B(C_6F_5)_4$ with dioxygen.[14] Fitting the observed spectral changes (Figure 1) to the simplest, sequential model of **1**⇌**2**⇌**3** (Scheme S1) yields spectra that are inconsistent with the absorption spectra of a pure *trans*-peroxo or bis-μ-oxo species (Figure S1). Inclusion of an additional pathway where **1** can also convert directly to **3** in a parallel kinetic model (Scheme 1) remedies the kinetically derived spectra

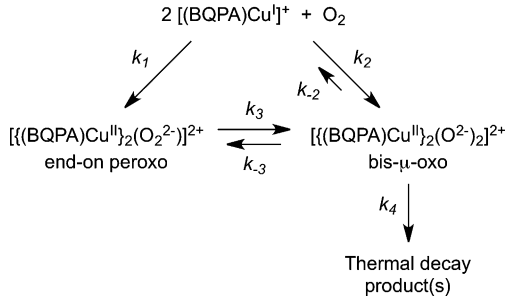

Scheme 1. Parallel kinetic model.

(Figure S1). While both species form simultaneously at the very early stages of the reaction, the formation of the *trans*-peroxo is preferred by an order of magnitude (i.e., $k_1 > k_2$) and at equilibrium roughly 85% of **3** is formed from **2**. As indicated in Scheme 1 and substantiated by the corresponding Eyring plots with varying initial concentrations of $[(BQPA)Cu^{I}]^+$ (**1**) and O_2 (Figure S2), these initial reactions are second order in **1** and first order in O_2 for both the formation of **2** and **3**. Subsequently, **2** is converted in a first order reaction (k_3) to the more thermodynamically stable bis-μ-oxo species **3**; this transformation is zero order in $[(BQPA)Cu^{I}]^+$. The same is true for the back reaction k_{-3} from **3** to **2** ($K_{EQ} = k_3/k_{-3} = 3.2$ at −90 °C; Table 1). Further, thermodynamic parameters for the parallel kinetic model (Scheme 1) were determined

Table 1: Rates and thermodynamic parameters for the reactions in Scheme 1.

	k (−90 °C)	$\Delta H^{\ddagger}$ [kcal mol^{-1}]	$\Delta S^{\ddagger}$ [cal mol^{-1} K]
k_1 [$M^{-2}s^{-1}$]	$(4.3\pm0.4)\times10^{5}$	-1.4 ± 0.1	-39.4 ± 0.5
k_2 [$M^{-2}s^{-1}$]	$(5.9\pm0.2)\times10^{4}$	-1.9 ± 0.2	-46 ± 1
k_{-2} [s^{-1}]	$(3\pm2)\times10^{-5}$	17.0 ± 0.5	15 ± 3
k_3 [s^{-1}]	$(1.6\pm0.1)\times10^{-1}$	10.94 ± 0.05	-1.4 ± 0.2
k_{-3} [s^{-1}]	$(5.0\pm0.2)\times10^{-2}$	10.29 ± 0.05	-7.2 ± 0.2

indicating that the formation of the bis-μ-oxo from the *trans*-peroxo is slightly exergonic ($\Delta H = -0.64\pm0.07$ kcal mol^{-1}, $\Delta S = 5.7\pm0.3$ cal mol^{-1} K).

We sought to computationally model these thermodynamic results by surveying the functional dependence of the end-on peroxo/bis-μ-oxo equilibrium. We also included a series of related copper–dioxygen adducts in the modeling, since TMPA and BPQA yield *trans*-peroxo species as the thermodynamic product while Me_2tpa (like BQPA) yields a bis-μ-oxo as the thermodynamic product (Figure 2).[8,9,11] Of the tested methods, BLYP, BP86, mPWPW91, PBE, and TPSSh correctly predicted Me_2tpa and BQPA to form bis-μ-oxo species and for BPQA and TMPA, end-on peroxo adducts were energetically favored.

This calibrated computational methodology was then applied to the binuclear "end-on" copper-dioxygen complex $[Cu_2(O_2)(m\text{-}Xyl^{N3N4})]^{2+}$ (**4**) (Figure 2) that was recently reported to perform the *ortho*-hydroxylation of 4-methyl-phenolate.[5] Attribution of this electrophilic reactivity to an end-on peroxo core is significant because it contradicts a sizeable pool of literature that suggests this structural type displays nucleophilic reactivity.[2d,4] These calibrated computational methods indicate that a bis-μ-oxo isomer of **4** is in fact energetically accessible. This is in contrast to the DFT calculations reported in reference [5] which suggested that a bis-μ-oxo isomer was approximately 40 kcal mol^{-1} higher in energy. Our calculations differed from the previous report in two major respects. First, using the computational methodology reported in reference [5], we found an alternative structure of the putative bis-μ-oxo species that was approximately 15 kcal mol^{-1} more favorable due to equatorial coordination of the amine ligand (Table S10). Second, the experimentally calibrated methodology developed in this report indicates that the bis-μ-oxo isomer of **4** is within 2 kcal mol^{-1} of the end-on peroxo isomer (Table S12). This is in contrast to the DFT methodology in reference [5] that predicts that the bis-μ-oxo is 25 kcal mol^{-1} higher than the end-on peroxo. Thus while experimental data in reference [5] indicate that **4** is an end-on peroxo, the calibrated DFT calculations presented here indicate that a bis-μ-oxo isomer is energetically accessible.[15] The reaction coordinate for electrophilic aromatic substitution of 4-methyl-phenolate was thus revaluated using the improved ligand geometries and calibrated method (TPSSh is shown in Figure 7). The bis-μ-oxo was found to have both a larger driving force and a lower barrier to *ortho*-hydroxylation than the end-on peroxo despite being slightly higher in energy in the absence of an interaction with 4-methylphenolate (2 kcal mol^{-1}). Our present experimental findings with BQPA provide precedent that

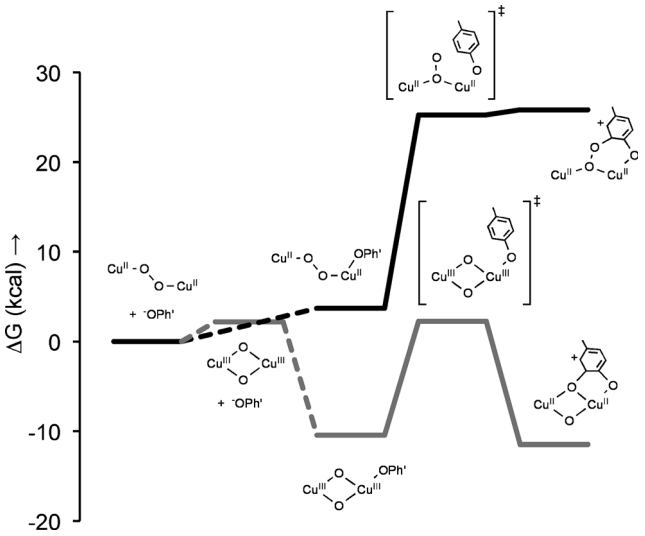

Figure 7. Computational evaluation of electrophilic aromatic substitution by a end-on peroxo (black curve) and bis-μ-oxo (gray curve) of **4**.

the end-on species **4** can convert to a bis-μ-oxo species, which is computationally capable of performing the electrophilic aromatic substitution observed experimentally for the *m*-Xyl^{N3N4} system.

In conclusion, analysis of the oxygenation of $[(BQPA)Cu^{I}]^{+}$, utilizing rR spectroscopy, kinetics analyses, and DFT calculations has led to the observation of an end-on peroxo/bis-μ-oxo equilibrium, featuring formation of the end-on peroxo isomer followed by its conversion to the thermodynamically more stable bis-μ-oxo species (Scheme 1, $K_{eq} = 3.2$ at −90 °C); a first in transition metal–dioxygen chemistry. This equilibrium sheds light on the reactivity patterns in Cu_2O_2 chemistry, and strongly suggests that the nucleophilic reactivity pattern of end-on peroxo species holds, in contrast to the recent literature wherein electrophilic reactivity has been proposed.

Experimental Section

BQPA was synthesized as previously reported[7] and metalated with $[Cu^{I}(CH_3CN)_4]B(C_6F_5)_4$ to form $[Cu^{I}(BQPA)](BC_6F_5)_4$ (see Supporting Information). Low-temperature stopped-flow kinetics were carried out as previously described and for numerical analysis, all data were pretreated by factor analysis and concentration profiles were calculated by numerical integration.[8,16] rR samples were prepared by adding dioxygen to solutions of $[Cu^{I}(BQPA)](BC_6F_5)_4$ in dry, degassed THF (see Supporting Information for details). DFT calculations were performed using Gaussian03.[17] Molecular structures were optimized using the B3LYP functional within the spin-unrestricted formalism on an ultrafine integration grid. The basis sets employed on Cu, O, and N were of triple-ζ quality with polarization (6-311g*). A double-ζ quality, split-valence basis was used on all other atoms (6-31g*). The functional dependence of the end-on peroxo/bis-μ-oxo equilibrium was determined from solvated single-point energies (PCM model in THF) for the tested functionals (BLYP, BP86, mPWPW91, PBE, TPSSh, B3LYP, BMK, M06, M06L, mPW1PW91, τHCTH, TPSS, VSXC) with the same basis set and B3LYP thermal correction at −80 °C.

Received: February 6, 2014
Published online: April 2, 2014

Keywords: copper · dioxygen ligands · Raman spectroscopy · structure–function relationship · tyrosinase

[1] a) E. I. Solomon, D. E. Heppner, E. M. Johnston, J. W. Ginsbach, J. Cirera, M. Qayyum, M. T. Kieber-Emmons, C. H. Kjaergaard, R. G. Hadt, L. Tian, *Chem. Rev.* **2014**, DOI: 10.1021/cr400327t; b) J. W. Ginsbach, M. T. Kieber-Emmons, R. Nomoto, A. Noguchi, Y. Ohnishi, E. I. Solomon, *Proc. Natl. Acad. Sci. USA* **2012**, *109*, 10793 – 10797.

[2] a) N. Kitajima, Y. Moro-oka, *Chem. Rev.* **1994**, *94*, 737 – 757; b) L. M. Mirica, X. Ottenwaelder, T. D. P. Stack, *Chem. Rev.* **2004**, *104*, 1013 – 1045; c) E. A. Lewis, W. B. Tolman, *Chem. Rev.* **2004**, *104*, 1047 – 1076; d) L. Q. Hatcher, K. D. Karlin, *J. Biol. Inorg. Chem.* **2004**, *9*, 669 – 683.

[3] a) M. S. Nasir, B. I. Cohen, K. D. Karlin, *J. Am. Chem. Soc.* **1992**, *114*, 2482 – 2494; b) E. Pidcock, H. V. Obias, C. X. Zhang, K. D. Karlin, E. I. Solomon, *J. Am. Chem. Soc.* **1998**, *120*, 7841 – 7847; c) P. L. Holland, K. R. Rodgers, W. B. Tolman, *Angew. Chem.* **1999**, *111*, 1210 – 1213; *Angew. Chem. Int. Ed.* **1999**, *38*, 1139 – 1142; d) L. M. Mirica, M. A. Vance, D. J. Rudd, B. Hedman, K. O. Hodgson, E. I. Solomon, T. D. P. Stack, *Science* **2005**, *308*, 1890 – 1892; e) A. Company, S. Palavicini, I. Garcia-Bosch, R. Mas-Balleste, L. Que, E. V. Rybak-Akimova, L. Casella, X. Ribas, M. Costas, *Chem. Eur. J.* **2008**, *14*, 3535 – 3538; f) M. F. Qayyum, R. Sarangi, K. Fujisawa, T. D. P. Stack, K. D. Karlin, K. O. Hodgson, B. Hedman, E. I. Solomon, *J. Am. Chem. Soc.* **2013**, *135*, 17417 – 17431.

[4] P. P. Paul, Z. Tyeklár, R. R. Jacobson, K. D. Karlin, *J. Am. Chem. Soc.* **1991**, *113*, 5322 – 5332.

[5] I. Garcia-Bosch, A. Company, J. R. Frisch, M. Torrent-Sucarrat, M. Cardellach, I. Gamba, M. Güell, L. Casella, L. Que, Jr., X. Ribas, J. M. Luis, M. Costas, *Angew. Chem.* **2010**, *122*, 2456 – 2459; *Angew. Chem. Int. Ed.* **2010**, *49*, 2406 – 2409.

[6] a) D. Maiti, J. S. Woertink, A. A. Narducci Sarjeant, E. I. Solomon, K. D. Karlin, *Inorg. Chem.* **2008**, *47*, 3787 – 3800; b) H. R. Lucas, L. Li, A. A. N. Sarjeant, M. A. Vance, E. I. Solomon, K. D. Karlin, *J. Am. Chem. Soc.* **2009**, *131*, 3230 – 3245.

[7] N. Wei, N. N. Murthy, Q. Chen, J. Zubieta, K. D. Karlin, *Inorg. Chem.* **1994**, *33*, 1953 – 1965.

[8] K. D. Karlin, N. Wei, B. Jung, S. Kaderli, P. Niklaus, A. D. Zuberbuhler, *J. Am. Chem. Soc.* **1993**, *115*, 9506 – 9514.

[9] R. R. Jacobson, Z. Tyeklar, A. Farooq, K. D. Karlin, S. Liu, J. Zubieta, *J. Am. Chem. Soc.* **1988**, *110*, 3690 – 3692.

[10] a) Z. Tyeklar, R. R. Jacobson, N. Wei, N. N. Murthy, J. Zubieta, K. D. Karlin, *J. Am. Chem. Soc.* **1993**, *115*, 2677 – 2689; b) M. J. Baldwin, P. K. Ross, J. E. Pate, Z. Tyeklar, K. D. Karlin, E. I. Solomon, *J. Am. Chem. Soc.* **1991**, *113*, 8671 – 8679.

[11] H. Hayashi, S. Fujinami, S. Nagatomo, S. Ogo, M. Suzuki, A. Uehara, Y. Watanabe, T. Kitagawa, *J. Am. Chem. Soc.* **2000**, *122*, 2124 – 2125.

[12] In an earlier kinetic analysis,[8] it was suggested that a cupric superoxo species was formed following the end-on peroxo species. At this time, a $Cu^{III}_2(\mu\text{-oxo})_2$ species had not been discovered.

[13] a) Y. Lee, G. Y. Park, H. R. Lucas, P. L. Vajda, K. Kamaraj, M. A. Vance, A. E. Milligan, J. S. Woertink, M. A. Siegler, A. A. Narducci Sarjeant, L. N. Zakharov, A. L. Rheingold, E. I. Solomon, K. D. Karlin, *Inorg. Chem.* **2009**, *48*, 11297 – 11309; b) Y. Lee, D.-H. Lee, G. Y. Park, H. R. Lucas, A. A. Narducci

Sarjeant, M. T. Kieber-Emmons, M. A. Vance, A. E. Milligan, E. I. Solomon, K. D. Karlin, *Inorg. Chem.* **2010**, *49*, 8873 – 8885.
[14] An initial report on the solution kinetics and the equilibrium was published in a meeting abstract, see P. K. Wick, K. D. Karlin, M. Suzuki, A. D. Züberbuhler, *Micron* **2004**, *35*, 137 – 139.
[15] While one might expect that an energetically accessible bis-μ-oxo isomer in **4** would oxygenate thioanisol, no reaction was previously observed.[5] This lack of this reactivity may be complicated by the coordination of thioanisol in the open coordination site in **4**, stabilizing the end-on peroxo isomer relative to the bis-μ-oxo.
[16] a) K. D. Karlin, M. S. Nasir, B. I. Cohen, R. W. Cruse, S. Kaderli, A. D. Zuberbuhler, *J. Am. Chem. Soc.* **1994**, *116*, 1324 – 1336; b) C. X. Zhang, S. Kaderli, M. Costas, E. Kim, Y. M. Neuhold, K. D. Karlin, A. D. Zuberbuhler, *Inorg. Chem.* **2003**, *42*, 1807 – 1824; c) K. D. Karlin, C. X. Zhang, A. L. Rheingold, B. Galliker, S. Kaderli, A. D. Zuberbühler, *Inorg. Chim. Acta* **2012**, *389*, 138 – 150.
[17] M. J. Frisch, et al., Gaussian 03, revision E.01; Gaussian, Inc.: Wallingford, CT, **2004**.

